Ablation behaviour of interpenetrating Al/graphite composites

LIANMEI WU[a], GAOHUI WU[b,*], BINGQING LI[b], PENGCHAO KANG[b], SU CHEN[b], WENSHU YANG[b]
[a]*Beijing Institute of Electronic System Engineering, Beijing, 100854, China*
[b]*School of Materials Science and Engineering, Harbin Institute of Technology, Harbin 150001, China*

Interpenetrating Al/graphite composites were fabricated by vacuum pressure infiltration technique. The ablation performance was evaluated by an arc-heater. After the addition of Al, the linear ablation rate decreased by one order of magnitude. At the beginning of the ablation, Al inside the composite near the ablation surface rapidly liquefied and evaporated, which helped to decrease the temperature rise inside the composites. Then the liquid or evaporated Al was oxidized to form a liquid Al_2O_3 layer on the ablation surface to protect the composites from further ablation. Thus the ablation resistance of the composite was greatly improved.

(Received March 16, 2014; accepted March 19, 2015)

Keywords: Interpenetrating Al/graphite composites, Aerospace materials, Oxidation, Ablation mechanism

1. Introduction

The temperature of the leading edges of the future hypersonic vehicles may exceed 2000°C during the re-entry process [1]. Therefore, it is imperative to develop refractory materials with non-ablative properties [2]. Three different materials have been considered: refractory metals, C/C composites and ultra-high temperature ceramics (UHTCs).

Though refractory metals are widely used in the aerospace field, they are not suitable for the hypersonic applications due to their high density [3]. C/C composites are very promising due to their outstanding high temperature strength, good thermal shock resistance and low density. However, it cannot be utilized above 500°C without any protection due to its poor oxidation resistance [4]. Several coatings, such as SiC, HfC, TaC, ZrC, have been developed to protect C/C from ablation [6]. During the ablation, the coatings turns to liquid oxides covered on the ablation surface, which hinders further oxidation. However, their applications are also limited due to the lack of economical processing methods [5].

Among the UHTCs, ZrB_2 based ceramics have attracted much attention because of their excellent mechanical and chemical stability at high temperature [7]. In the past, substantial progress has been achieved in fabrication, characterization and toughening of ZrB_2-based composites [8]. The addition of SiC particles improves the densification of ZrB_2 by maintaining a fine grain size and a uniform distribution of the reinforcing phase. Besides, the oxidation resistance can be enhanced by the formation of the Si-B-O glass that inhibits oxidation between 800 and 1700°C [9]. However, the thermal shock resistance of the UHTCs is the technical bottleneck which still needs further improvement.

It can be known from the above discussion that the liquid oxide layer on the ablation surface plays an important role in resisting ablation. Therefore, the effect of the oxide layer on the ablation behaviour of the graphite was investigated in this work. In order to get a fast formation of the oxide layer during ablation, light reductive metal Al with low melting and evaporating temperature was chosen to infiltrate into the porous graphite. The ablation behaviour and ablation mechanism of Al/graphite composites were investigated.

2. Material and methods

G176 graphite (Harbin electric carbon company, China) with a density of 1.7g/cm^3 and an open porosity of about 20.6 vol.% was used as the preform. Al was infiltrated into the graphite pores by vacuum pressure infiltration method [11].

Three samples with dimension of Φ 15×45 mm were used for each ablation time. The ablation was performed on an arc-heater. The stagnation pressure, the heat flux, and the ablation temperature were 2.5atm, 4MW/m^2 and 2300°C, respectively. The linear ablation rate (R_d) is defined as:

$$R_d=\Delta d/t \quad (1)$$

where Δd is the length change after the ablation and t is the ablation time.

The microstructure and the phase constitution of the composite were examined by S-4700 scanning electron microscopy (SEM, Hitachi, Japan) and X-ray diffraction (XRD, Rigaku D/max-rB, Japan), respectively.

3. Results and discussion

3.1 Ablation properties

Fig. 1 presents the linear ablation rate of the graphite and the composite for the different length of times. In the first 5s, the linear ablation rate of the graphite is 4.8×10^{-2} mm/s, while that of the composite decreases by one order of magnitude and is only -4.2×10^{-3} mm/s. The ablation resistance of the composite is greatly improved after infiltrating Al. The linear ablation rate varies little with time during the whole ablation process. After undergoing 40s ablation, the linear ablation rate of the composite is 5.2×10^{-3} mm/s, decreasing by 93% compared with that of the graphite. So it is obvious that the ablation properties of the composite are determined by Al.

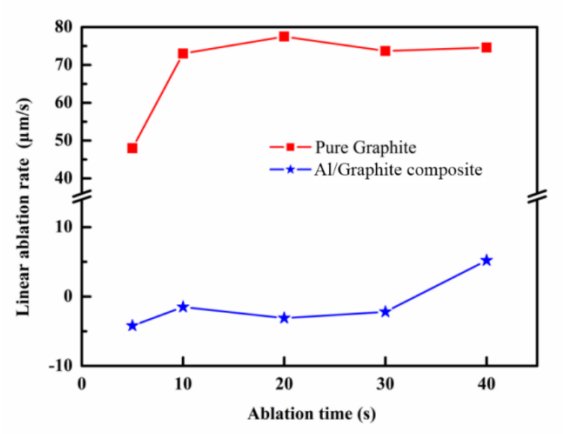

Fig. 1. The linear ablation comparison between composite and graphite.

3.2 Microstructure characterization

Representative morphologies of the graphite and the composites are shown in Fig. 2. Large amount of pores exist in the graphite substrate (Fig. 2a). In Fig. 2b, the bright areas correspond to Al and the dark areas are graphite. It can be seen that Al fills the graphite pores uniformly and presents network structure, which is beneficial to the formation of a continuous alumina coating during the ablation.

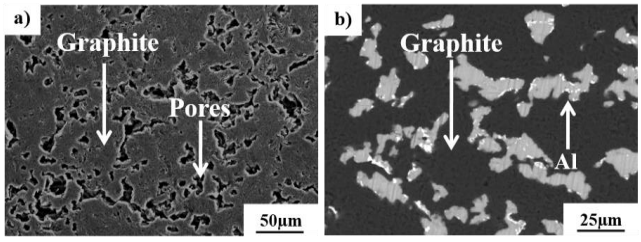

Fig. 2. The microstructure of the graphite a) and Al/graphite composites b).

Fig. 3 shows the surface morphology of the graphite after 40s ablation. The microstructure of the graphite turns to be loose after undergoing 40s ablation. The thermochemical ablation preferentially occurs at the defects in the graphite, leading to a weak binding between the graphite grains. Then the graphite grains are easily denudated by the ablation environment and the graphite presents loose structure. Fig. 4 presents the macro surface morphology, the micro section morphology and the XRD result of the ablation surface. It can be seen from Fig. 4a that a glass layer covers on the ablation surface. Further observation in Fig. 4b and Fig. 4c demonstrates that the glass layer is α-Al_2O_3 with average thickness of 60μm. The α-Al_2O_3 layer, as an efficient barrier for oxygen diffusion and heat transfer, can prevent further ablation of the composite.

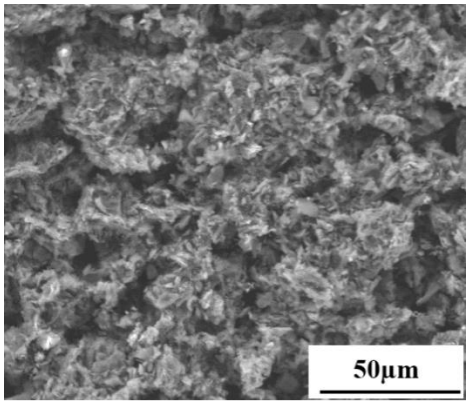

Fig. 3. The surface morphology of the graphite after 40s ablation.

The ablation surface can be divided into three different regions: central region (Ⅰ), transition region (Ⅱ) and border region (Ⅲ), as shown in Fig. 4a. The corresponding micro-morphologies are presented in Fig. 5. In central region (Fig. 5a), some pores with diameter of about 20μm for the escape of vaporized Al are observed (Fig. 5b). In transition region, the coating is less dense than that in central region and more pores are found (Fig. 5c). It is worth noting that the morphology in transition zone presents river patterns (Fig. 5c and Fig. 5d). The microstructure in border region is droplet-like (Fig. 5e and Fig. 5f), which indicates that molten Al_2O_3 is flowed under high-speed airflow at high temperature.

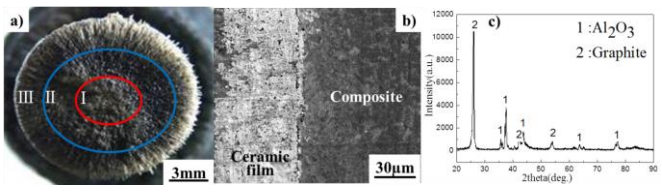

Fig. 4. The surface a) and section b) ablation morphology of the central zone with the corresponding XRD result c) after the ablation for 40 s.

3.3 Ablation mechanism

During the ablation at 2300ºC, the heat is dissipated through a series of endothermic processes, for instance, the melting and the evaporating of Al and Al_2O_3. Thus, the temperature rise in the composite is restrained and the ablation resistance gets enhanced.

At the beginning of the ablation, the graphite and Al near the ablation surface are oxidized to CO_2 and Al_2O_3, respectively. Al beneath the ablation surface gradually liquefies, evaporates and then diffuses outward the surface layer. The liquid or evaporated Al continuously oxidizes to Al_2O_3 to form protective coating (Fig. 5b). The reactions are believed to occur as follows:

$$4Al(l/g) + 3O_2(g) \rightarrow 2Al_2O_3(l) \quad (2)$$

$$2C(s) + O_2(g) \rightarrow 2CO(g) \quad (3)$$

$$2CO(s) + O_2(g) \rightarrow 2CO_2(g) \quad (4)$$

Furthermore, Al_2O_3 is liquid since its melting point (2054 ºC) is lower than the environment temperature (2300 ºC). The liquid Al_2O_3 on the surface provides a self-sealing mechanism to fill the interspaces, cracks and pores in matrix. The oxygen diffusion to the underlying material is then restrained. Meanwhile, Al_2O_3 also decreases the heat transfer due to its low thermal conductivity and acts as a thermal barrier. Moreover, the molten Al_2O_3 can slight the mechanical denudation. Therefore, the ablation resistance is improved efficiently.

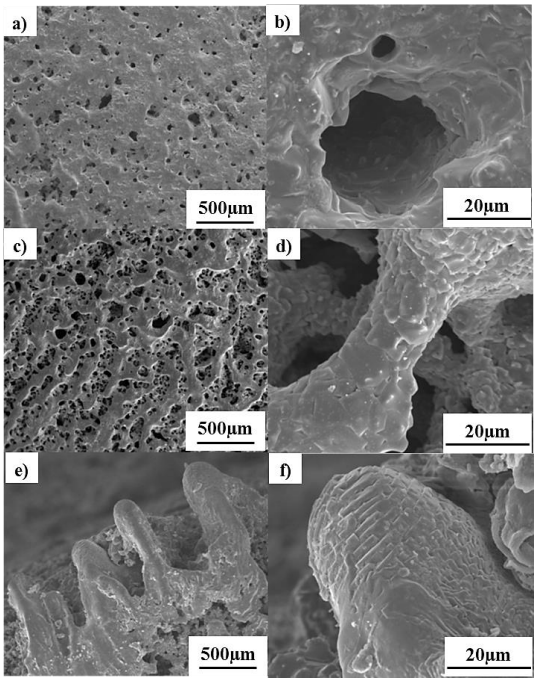

Fig. 5. SEM results of the composite after 40s ablation: central region (a, b), transition region (c, d) and border region (e, f).

4. Conclusions

In conclusion, the addition of Al to graphite can greatly improve the ablation resistance. At high temperature (> 2054 ºC), liquid Al_2O_3 provides a self-sealing mechanism to obstruct oxygen diffusion. Meanwhile, the low thermal conductivity of Al_2O_3 decreases the heat transfer. Under these coupling mechanisms, the linear ablation rate of Al/graphite composite varies little with time and is only 5.2×10^{-3} mm/s after 40s ablation.

Acknowledgments

This work is supported by National Natural Science Foundation of China (90816017).

References

[1] S. Biamino, V. Liedtke, C. Badini, G. Euchberger, I. H. Olivares, M. Pavese, P. Fino, Journal of the European Ceramic Society, **28**, 2791 (2008).
[2] J. C. Han, P. Hu, X. H. Zhang, S. H. Meng, W. B. Han, Composites Science and Technology. **68**, 799 (2008).
[3] J. M. Su, L. Q. Chen, S. X. Wang, X. Hou, G. L. Li, Journal of Solid Rocket Technology, **27**, 69 (2004).
[4] H. Mayer, M. Papakyriacou, Carbon, **44**, 1801 (2006).
[5] T. Etter, P. Schulz, M. Weber, J. Metz, M. Wimmler, J. F. Loffler, P. J. Uggowitzer, Materials Science and Engineering A **448**, 1 (2007).
[6] X. T. Li, J. L. Shi, G. B. Zhang, H. Zhang, Q. G. Guo, L. Liu, Materials Letters, **60**, 892 (2006).
[7] G. M. Song, S. B. Li, C. X. Zhao, W. G. Sloof, S. V. D. Zwaag, Y. T. Pei, J. T. M. D. Hosson, Journal of the European Ceramic Society, **31**, 855 (2011).
[8] J. C. Han, P. Hu, X. H. Zhang, S. H. Meng, Scripta Materialia, **57**, 825 (2007).
[9] Z. Wang, S. Wang, X. H. Zhang, P. Hu, W. B. Han, C. Q. Hong, Journal of Alloys and Compounds, **484**, 390 (2009).
[10] G. H. Wu, X. Liu, S. Chen, L. M. Wu, X. Bai, Aerospace Materials & Technology, **1**, 32 (2010).
[11] G. H. Wu, S. Chen, Q. Zhang, China, ZL200810064995.2.

*Corresponding author: wugh_hit@163.com